Monatsh Chem (2010) 141:101–109
DOI 10.1007/s00706-009-0232-5

ORIGINAL PAPER

Lipid- and water-soluble bilirubins

Sanjeev K. Dey · David A. Lightner

Received: 15 October 2009 / Accepted: 22 November 2009 / Published online: 19 January 2010

Abstract Novel bilirubin analogs with two nonionic, water-solubilizing polyethyleneglycol (PEG) β-substituents of varying chain length on the lactam ring of each dipyrrinone were synthesized. In contrast to bilirubin, which is insoluble in CH_3OH and in H_2O at pH 7 but somewhat soluble in $CHCl_3$ ($\sim$1 mM), the PEGylated rubins are soluble in all three solvents, with H_2O solubility increasing with increasing number of ethyleneglycol units in the PEG chain(s). Vapor pressure osmometry indicates that, like bilirubin, they are monomeric in $CHCl_3$ and in CH_3OH. Nuclear magnetic resonance (NMR) studies indicate that their most stable structure in these solvents and in H_2O has the 4*Z*,15*Z* configuration that is bent into a ridge-tile shape with the pigment's dipyrrinones engaged in intramolecular hydrogen bonding to the propionic acid carboxyl groups. Aqueous pK_a values for the intramolecularly hydrogen-bonded carboxyl groups of these compounds, determined by vacuum-assisted multiplexed capillary electrophoresis in H_2O–CH_3OH mixtures followed by Yesuda-Shedlovsky extrapolations to pure H_2O, were found to be 4.9, as previously determined by NMR titrations for mesobilirubin-XIIIα.

Keywords Tetrapyrrole · Polyethyleneglycol · NMR · pK_a

S. K. Dey · D. A. Lightner (✉)
Department of Chemistry, University of Nevada,
Reno, NV 89557-0216, USA
e-mail: lightner@scs.unr.edu

Introduction

Bilirubin (Fig. 1a), the yellow neurotoxic pigment of jaundice [1–3] and the end product of heme metabolism in mammals [1–3], is a water-insoluble, lipophilic tetrapyrrole dicarboxylic acid [2, 3]. Produced copiously in healthy humans by enzymic reduction of its blue-green biogenetic precursor, biliverdin, formed by catabolism of heme (Fig. 1a) and other heme proteins, it is eliminated from circulation by crossing the liver into bile [1, 4, 5]. Unlike biliverdin, which is polar and excreted intact across the liver, bilirubin is nonpolar and requires glucuronidation of at least one propionic acid group for transhepatic transport [1]. We now know that biliverdin, which has a 4*Z*,10*Z*,15*Z* configuration, adopts a porphyrin-like conformation [6], whereas the most stable conformation of (4*Z*,15*Z*)-rubins is neither linear nor porphyrin-like, but shaped like a ridge-tile [7]. In bilirubin the two dipyrrinones may in principle rotate freely about the central CH_2 at C(10) to generate a multitude of conformations, of which the linear and porphyrin-like are highest energy, and that resembling a half-opened book (Fig. 1b) minimizes intramolecular nonbonded steric repulsions [7]. The ridge-tile conformation of bilirubin (Fig. 1b) is stabilized by intramolecular hydrogen bonds between the propionic acid COOH groups and the opposing dipyrrinone lactam and pyrrole groups [7–12], a conformation that explains its lipophilicity and considerable water insolubility ($K_{sp} \sim 4 \times 10^{-15}$ at pH 7) [13, 14] and correlates with the pigment's inability to be excreted intact by the liver [1–3].

Earlier, we explored the influence of nonionizable substituents on the lipophilicity of bilirubins, while retaining intramolecular hydrogen bonding. We thus designed and synthesized analogs that were capable of intramolecular

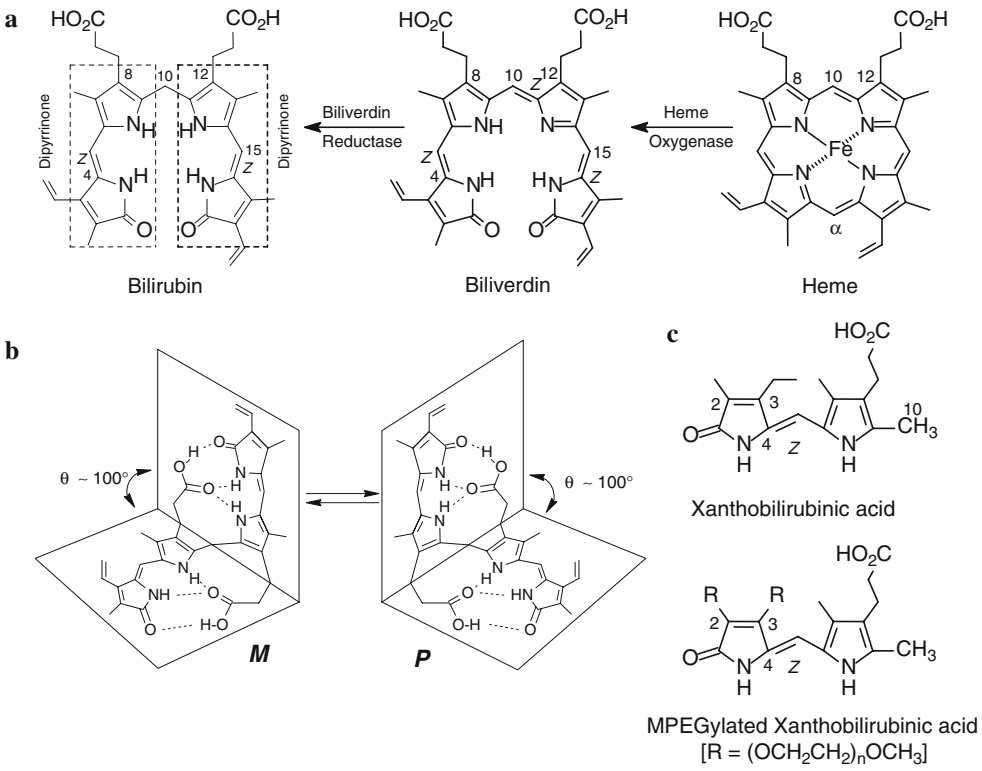

Fig. 1 **a** Formation of bilirubin via biliverdin (shown in porphyrin-like representations) from catabolism of heme. **b** The most stable conformation of bilirubin is neither linear nor porphyrin-like but folded into a half-opened book or ridge-tile shape that is stabilized by six intramolecular hydrogen bonds (shown as two interconverting conformational enantiomers). In contrast, the most stable conformation of biliverdin is porphyrin-like and helical. **c** Xanthobilirubinic acid (*upper*) and its 2,3-PEGylated analogs (*lower*) having improved aqueous solubility as *n* goes from 0 to 3

hydrogen bonding but were more lipophilic than bilirubin by: (1) changing the lactam *β*-substituents from methyl and vinyl to ethyls [15, 16], and to a methyl and *n*-butyl [17], which increased the pigment's lipophilicity; and (2) adding a *gem*-dimethyl group to C(10), which increased the pigment's solubility in nonpolar as well as polar (e.g., CH_3OH) solvents [15, 16]. Particularly relevant to the current study is the synthesis of a water-soluble bilirubin with one polyethyleneglycol (PEG) covalently attached. The pigment's intramolecular hydrogen-bonding ability and intrinsic lipophilicity remained unperturbed [18], but in water at pH <10, it was found to be aggregated, probably with the pigment units sequestered in the core of a PEG micelle. To avoid aggregation, we initiated the syntheses of new PEGylated bilirubins with more but shorter polyether *β*-substituents on the pigment's lactam rings. Thus, 2,18-di(desmethyl)-3,17-di(desvinyl)-2,3,17,18-tetramethoxybilirubin was prepared as the "parent" and found to have slightly improved methanol solubility [19]. This promising result led to our recent investigations of xanthobilirubinic acids (Fig. 1c) modified to include short polyethyleneglycol methyl ether (MPEG) chains on the lactam ring [20]. The most promising of these modified xanthobilirubinic acids had the longest (triethyleneglycol methyl ether) chain studied and was water soluble. In the following, we report the preparation of tetra-MPEGylated bilirubins **1**–**3** (Fig. 2) and compare their properties with those of the tetramethoxy analog **4** and bilirubin.

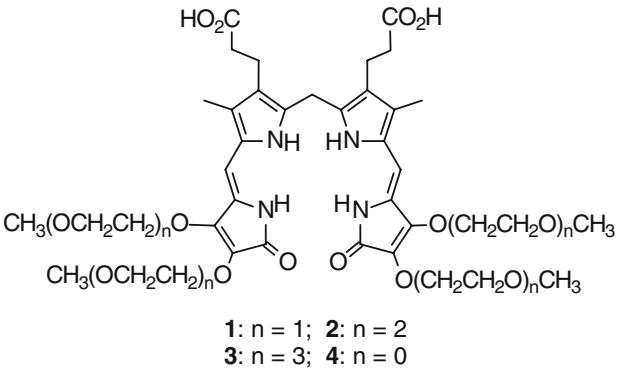

Fig. 2 The target PEGylated bilirubinoids of this work

Results and discussion

Synthesis aspects

From our perspective, the simplest route to the preparation of **1**–**3** was to follow the "1 + 2 + 1" approach [21, 22] outlined in Scheme 1. Here an α,α′-diformyldipyrrylmethane is coupled with two equivalents of a pyrrolin-2-one [23, 24]. The strategy has been used successfully in the syntheses of various end ring-modified bilirubins [15, 23, 24] and (more recently) rubin **4** [19]. The syntheses of **1**–**3** required dipyrrole dialdehyde **5**, which had been reported previously [23, 24], and 3,4-MPEGylated pyrrolinones **6**–**8**, which were available in our laboratory and had been

Scheme 1

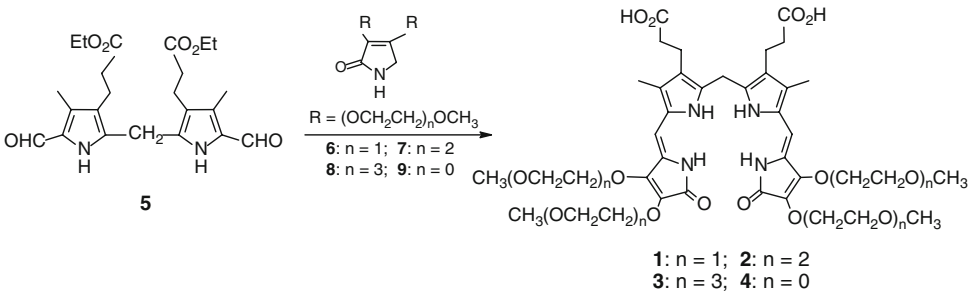

prepared recently in connection with other work [20]. Previously, condensation of dimethoxypyrrolinone **9** with **5** in refluxing methanolic KOH afforded **4** in 46% isolated yield, based on recovered tripyrrole intermediate [19]. Similar reactions of **5** with **6**–**9** were much less successful due to hydroxide-catalyzed elimination of the PEGylated substituents, and so other reaction conditions were developed using the same "1 + 2 + 1" approach. At this final synthetic step, which proved to be capricious, numerous modifications were tried: morpholine in refluxing CH_3OH–CH_3CN; piperidine in hot CH_3CN; phosphazene P_1-*t*-butyl in hot CH_3CN-toluene at reflux; and DBU in CH_3CN at 120 °C (sealed tube). The latter worked best when the reaction was carried out over 10 days, and at a lower temperature (120–130 °C). The yields were low at best, but the structures are well characterized. Carrying out the reactions at higher temperature, e.g., 150 °C, or over a longer time (more than 10 days) led to product decomposition and even lower yields.

Structure and ^{13}C NMR spectra

The constitutional structures of **1**–**3** follow from the components used and method of synthesis (Scheme 1) and from their ^{13}C NMR spectra (Table 1). When compared with ^{13}C NMR data from the known tetramethoxybilirubin **4** and mesobilirubin-XIIIα (MBR), the various ring carbons of the dipyrrinone(s) of **1**–**3** are found to have counterparts in **4** and even MBR with recognizably similar chemical shifts. As in the earlier comparison of **4** and 2,3,17,18-tetraethylbilirubin [19], major differences between **1**–**3** and MBR are found in the more shielded lactam ring carbons 1, 2, and 4 and C(5) of the former relative to the latter, the presence of multiple OCH_2 groups in **1**-**3**, and the deshielded OCH_2 and OCH_3 groups in the MPEG groups of **1**–**4**. Aside from the profusion of deshielded OCH_2 and OCH_3 groups of **1**, the ^{13}C NMR spectra are qualitatively rather similar to MBR.

Molecularity in solution by vapor pressure osmometry

Although the ridge-tile, intramolecularly hydrogen-bonded conformation of bilirubin is well established in nonpolar solvents such as $CHCl_3$, the limited solubility of bilirubin itself in $CHCl_3$ has so far thwarted vapor pressure osmometry (VPO) studies of its molecular weight in solution. However, analogs with increased solubility in $CHCl_3$, such as tetramethoxybilirubin **4** [25] and those with an *n*-butyl group on each lactam ring [17, 18] or a C(10) *gem*-dimethyl group [25], have been shown to be monomeric. In contrast, the more $CHCl_3$-soluble diethyl ester of bilirubin has been shown by VPO to be dimeric at concentration of

Table 1 ^{13}C NMR chemical shifts (δ, ppm) of **1**–**4** compared with mesobilirubin-XIIIα (MBR) in $CDCl_3$ at 23 °C

	Carbon[a]	1	2	3	4	MBR[b]
1, 19	C=O	169.3	169.4	169.4	166.0	171.9
2, 18	–C=	125.3	125.2	125.2	125.9	122.9
3, 17	–C=	147.6	147.7	147.6	146.3	147.1
4, 16	–C=	120.8	120.9	120.9	120.1	127.8
5, 15	–CH=	100.6	100.5	100.4	96.6	97.7
6, 14	–C=	124.1	124.0	124.1	121.4	122.4
7, 13	–C=	123.9	123.8	123.7	122.3	122.0
8, 12	–C=	119.4	119.3	119.3	119.1	119.3
9, 11	–C=	133.2	133.2	133.1	130.3	130.4
10	CH_2	22.4	22.4	22.4	23.5	23.3
$7^1/13^1$	CH_3	10.3	10.3	10.3	9.0	8.1
$8^1/12^1$	CH_2	18.7	18.7	18.7	19.2	19.2
$8^2/12^2$	CH_2	32.8	32.8	32.8	34.3	34.6
$8^3/12^3$	CO_2H	179.8	179.7	179.7	173.9	174.1

Assignments are based on gradient Heteronuclear Multiple Bond Correlation (gHMBC), gradient Heteronuclear Single Quantum Correlation (gHSQC) experiments, and nuclear Overhauser effect (NOE) measurements

Chemical shifts of alkoxy chains on C(2)/C(18) and C(3)/C(17) in order

1 2/18—($OCH_2CH_2OCH_3$): 71.3, 71.6, 59.3 ppm; 3/17—(OCH_2-CH_2OCH_3): 71.8, 71.5, 59.0 ppm

2 2/18—($OCH_2CH_2OCH_2CH_2OCH_3$): 71.4, 71.8, 70.3, 70.9, 59.3 ppm; 3/17—($OCH_2CH_2OCH_2OCH_3$): 72.1, 72.2, 70.2, 70.6, 59.2 ppm

3 2/18—($OCH_2CH_2OCH_2CH_2OCH_2CH_2OCH_3$): 71.4, 71.9, 70.3, 70.9, 70.95, 70.79, 54.3 ppm; 3/16—($OCH_2CH_2OCH_2CH_2OCH_2$-CH_2OCH_3): 72.13, 72.14, 70.17, 70.66, 70.84, 70.75, 59.2 ppm

4 2/18—OCH_3: 60.2 ppm; 3/17—OCH_3: 59.0 ppm

[a] For carbon numbering system, see Fig. 1

[b] Data from Ref. [26]

Table 2 Molecular weights of **1–4** in $CHCl_3$ and CH_3OH from vapor pressure osmometry

Compound	Formula weight (FW) (g/mol)	Molecular weight (MW) (g/mol)[a]	
		$CHCl_3$	CH_3OH
1	800	792 ± 61	832 ± 61
2	976	950 ± 74	1,036 ± 94
3	1,150	1,116 ± 57	1,236 ± 102
4	624	625 ± 13	Insol[b]

The calibration standard was benzil: FW = 210 g/mol, MW = 220 ± 15 g/mol

[a] Measured over a concentration range of 1.6-6.1 mol/kg. These required concentrations were inaccessible for **1–4** in H_2O

[b] Insoluble at the concentration ($\sim 10^{-2}$ M) required for the measurement

$1–4 \times 10^{-3}$ [6], and the dimers were shown by ^{1}H NMR to be intermolecularly hydrogen bonded [6, 25].

In order to assess whether **1–4** are monomeric in $CHCl_3$ solution, we determined their molecular weights by VPO [25]. Thus, as shown in Table 2, all four bilirubinoids were monomers in $CHCl_3$ solutions up to $\sim 10^{-2}$ M. Here again, the ability to adopt the monomeric state (of aggregation) is in part due to the ability of the acid to form a tightly knit set of six intramolecular hydrogen bonds and the considerable solubility in $CHCl_3$. In contrast, bilirubinoid esters form intermolecular hydrogen bonds between the dipyrrinone units [6, 25].

Are pigments **1–4** aggregated in more polar solvents such as CH_3OH and H_2O? VPO measurements of **1–3** in CH_3OH indicate monomers, but tetramethoxyrubin **4** was insufficiently soluble in CH_3OH for the measurement. Nonetheless, the data reveal that in methanol, a polar, hydroxylic solvent, the MPEGylated rubins are not aggregated. Unfortunately, the most water soluble of the MPEGylated rubins (**3**) was still insufficiently soluble ($\sim 10^{-2}$ M required) for the measurement. The triethyleneglycol rubin **3** is just on the edge of sufficient aqueous solubility. Our studies suggest that a rubin with tetra- or pentaethyleneglycols attached should exhibit sufficient aqueous solubility for VPO studies. Nonetheless, these VPO measurements indicate that solubilization of a carefully designed amphiphilic bilirubinoid can be accomplished in a polar, hydroxylic solvent.

Solubility and polarity

Visually similar to bilirubin, **1–4** are yellow-orange solids that form yellowish solutions. In contrast, MBR is a bright-yellow solid. All four alkoxylated pigments (**1–4**) are very soluble in $CHCl_3$; 10^{-2} M solutions are easily made, whereas bilirubin solubility is $\sim 10^{-3}$ M at its saturation limit. Bilirubin is essentially completely insoluble in CH_3OH (~ 0 μM) [13, 14], but **1–4** exhibit increasing solubility with increasing MPEG chain length, e.g., the solubility of **4** at the saturation limit is 10.5 μg/cm^3 but **1–3** form 10^{-2} M solutions. Comparative solubility studies of **1–4** and bilirubin at saturation in pure H_2O reveal **1**: 2 μg/cm^3, **2**: 5 μg/cm^3, and **3**: 32 μg/cm^3, whereas **4** and bilirubin are completely insoluble. We had hoped for an even greater aqueous solubility of **3**, but found its solubility to be just below the higher concentration range needed for determination of its molecularity in water.

Like bilirubin, **1–4** are fully extracted from $CHCl_3$ solutions into 5% aq. NaOH. In contrast, they are only marginally extracted from $CHCl_3$ into 5% (or saturated) aq. $NaHCO_3$. The bicarbonate:$CHCl_3$ partition ratios are: 11:89 (**1**), 5:95 (**2**), 4:96 (**3**), 11:89 (**4**), and 3:97 (bilirubin). Apparently for **2** and **3**, while the aqueous solubility has improved, their solubility in $CHCl_3$ has improved even more.

Chromatographic comparison by thin-layer chromatography (TLC) and high-performance liquid chromatography (HPLC) indicate increased polarity of **1–4** relative to bilirubin. On silica gel TLC (eluent 4% by vol CH_3OH in CH_2Cl_2) the R_f values are 0.40 (**1**), 0.45 (**2**), 0.50 (**3**), 0.74 (**4**), and 0.85 (bilirubin). A slight increase in polarity is noted with increasing MPEG chain length in **3**→**4**, but a major increase is noted when comparing **1–3** with tetramethoxy **4**, whose polarity is close to that of bilirubin. In agreement with the greater polarity of **1–4** relative to bilirubin, reverse-phase HPLC shows faster retention times for **1–3**: 10.5 min (**1**), 9 min (**2**), 7.8 min (**3**), and ~14 min (**4**) versus 18 min (bilirubin). Again **4** behaves more like bilirubin than **1–3**, but one may note a progressive decrease in lipophilicity from **3** to **2** to **1**, as the (poly)ether chain length increases.

Conformation from ^{1}H NMR spectroscopy

Dipyrrinones are known to be avid participants in hydrogen bonding, preferably to carboxylic acids [26–28], and the ^{1}H NMR spectroscopic chemical shifts seen for **1–4** show good correlation with the picture of intramolecularly hydrogen-bonded conformations. Their dipyrrinone NH deshieldings near 10.2 (lactam) and 9.0 ppm (pyrrole) in $CDCl_3$ (Table 3) are very similar to those found in meso-bilirubin-XIIIα and bilirubin, where intramolecular hydrogen bonding between a dipyrrinone and a carboxylic acid lead to lactam and pyrrole NH chemical shifts of ~10.5 and ~9 ppm, respectively [26–28]. In contrast, in $CDCl_3$, intermolecularly hydrogen-bonded dipyrrinone dimers exhibit lactam and pyrrole NH chemical shifts of ~11 and ~10 ppm, respectively, whereas dipyrrinone monomers exhibit lactam and pyrrole NH chemical shifts of ~8 ppm [29].

Table 3 Comparison of the lactam and pyrrole NH chemical shifts (δ, ppm) and the COOH chemical shifts (δ, ppm) of **1–4** and meso-bilirubin-XIIIα (MBR) in $CDCl_3$ and $(CD_3)_2SO$

Rubin	$CDCl_3$ solvent			$(CD_3)_2SO$ solvent		
	Lactam NH	Pyrrole NH	CO_2H	Lactam NH	Pyrrole NH	CO_2H
1	10.21	9.00	13.07	9.56	10.26	11.86
2	10.20	8.99	13.13	9.78	10.32	11.91
3	10.19	9.00	13.13	9.70	10.29	11.88
4	10.22	9.00	13.12	9.56	10.26	11.86
MBR	10.57	9.15	13.62	9.72	10.27	11.87

δ in ppm downfield from $(CH_3)_4Si$ for sample concentrations 4×10^{-3} M at 22 °C

A chemical shift of ~9 ppm for the dipyrrinone pyrrole NH may thus be taken as diagnostic of intramolecular hydrogen bonding, and in Table 3 one finds a pyrrole chemical shift of 9.0 ppm for **1–4** as compared with the 9.15 ppm value seen in MBR. We attribute the ~0.35 ppm deshielding of the lactam NH of **1–4** relative to MBR to be due to the presence of the electronegative ether groups on the lactam ring. The deshielding of the CO_2H ^1H NMR resonance to ~13 ppm [7, 23, 24, 26–28] provides added support to our conclusion that **1–4** are hydrogen-bonded monomers and adopt a bilirubin-like intramolecularly hydrogen-bonded conformation (Fig. 1b).

Additional support for the folded, intramolecularly hydrogen-bonded conformation is found from $^1H\{^1H\}$-homonuclear NOE experiments of **1–4** in $CDCl_3$. As expected for dipyrrinones in the *syn-Z* conformation, NOEs are found between the pyrrole and lactam NHs, and between the C(5,15) olefinic hydrogens and the C(7,13) methyls and C(3,17) ethylenoxyls (Fig. 3). Only a faint NOE could be seen between the CO_2H and lactam NH, which suggests weaker hydrogen bonding in **1–4** than in MBR or in bilirubin. In $(CD_3)_2SO$, **1–4** exhibited many of the same NOEs seen above, characteristic of the *syn-Z* configuration of the dipyrrinones.

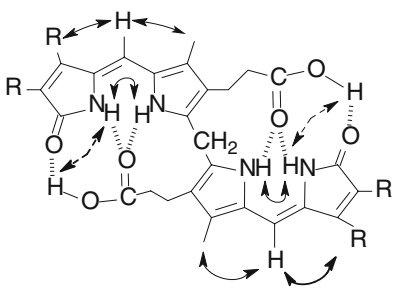

Fig. 3 Nuclear Overhauser effect correlations (*curved arrows*: strong, *solid curve*; weak, *dashed curve*) of **1–4** in $CDCl_3$

Consistent with intramolecularly hydrogen-bonded ridge-tile conformers (as in Fig. 1b) for **1–4** prevailing in $CDCl_3$, the ^1H NMR spectra (at 22 °C) show an *ABCX* splitting pattern for the $–CH_2–CH_2–$ segment of the propionic acid chains, as found in bilirubin [30] and various intramolecularly hydrogen-bonded bilirubinoids [15, 17, 19, 23, 24, 31, 32]. These observations correlate with a fixed staggered geometry in the propionic acid residues and a slow interconversion of conformational enantiomers (Fig. 1b) on the NMR timescale—an interconversion that requires breaking and remaking of at least three hydrogen bonds [7]. As in bilirubin, coalescence may be observed upon warming, and $\Delta G^{\ddagger}$ and the conformational enantiomer interconversion rate constant (k) may be derived (Table 4) from the coalescence temperature (T_c). From these data, we note similar $\Delta G^{\ddagger}$ and k for bilirubin and 2,17-di(desmethyl)-2,17-diethylmesobilirubin-XIIIα (tetraethylmesobilirubin [19]), with slightly lower values for **4**. The trend toward lower values continues from **1**→**3**, as the MPEG chains lengthen, yet throughout the data are consistent with the activation energy and rate constant associated with the interconversion of conformational enantiomers (Fig. 1b).

But do the ridge-tile conformations and intramolecular hydrogen bonds persist in CH_3OH and in H_2O? Although solubility limited our VPO studies to $CDCl_3$ and CH_3OH, we were able to measure the NH chemical shifts in H_2O using water-suppression techniques and found the lactam and pyrrole NH resonances at 9.75 and 8.95 ppm. Unfortunately we could not confirm the assignments nor measure NOEs between the NHs due to their somewhat broadened signals, nor could we see the splittings in the propionic acid $–CH_2–CH_2–$ segments, but it is probable that the higher field signal (8.95 ppm) is due to the pyrrole NH, and a pyrrole NH chemical shift of ~9 ppm has invariably signaled intramolecular hydrogen bonding in a ridge-tile conformation. Even in [6]-semirubin, an intramolecularly hydrogen-bonded dipyrrinone model for bilirubins, the pyrrole NHs are characteristically similarly shielded. Given

Table 4 Comparison of coalescence temperature (T_c), activation energy ($\Delta G^{\ddagger}$), and interconversion rate constants of **1–4** and 2,17-di(desmethyl)-2,17-diethylmesobilirubin-XIIIα (DEMBR) in $(CDCl_2)_2$ solvent

Compound	T_c (°C)	$\Delta G^{\ddagger}$ (kJ/mol)	k (s^{-1})
1	85	74.6	98
2	83	74.4	93
3	78	73.3	93
4	95	76.6	108
DEMBR	110	79.9	106
Bilirubin	105	78.7	109

these data, we conclude that **1**–**4**, like bilirubin, are intramolecularly hydrogen bonded in H_2O and probably also in CH_3OH, in the ridge-tile conformation, as they are in $CHCl_3$.

Conformation from UV–visible spectral analysis

Additional evidence on the conformation of **1**–**4** comes from solvent-dependent UV–Vis spectra. Over a wide range of solvents with varying polarity and hydrogen-bonding ability (benzene, chloroform, acetone, methanol, acetonitrile, and dimethylsulfoxide), the UV–Vis spectra of **1**–**4** show similar solvent dependence (Table 5), with broad absorption near 430 nm and a shoulder near 395 nm in most solvents. These long-wavelength absorptions are probably excitonic in nature [20] and correspond to the two exciton components from electric dipole–electric dipole transition moment interaction of the two dipyrrinone chromophores.

In exciton coupling theory, the relative orientation of the relevant electric dipole transition moments is very important [7, 33]. For dipyrrinones, this transition dipole lies along the long axis of the chromophore [34, 35]. The dipyrrinones may rotate into a large number of relative orientations (conformations), and the planes encompassing each dipyrrinone are not coincident; thus, the dipyrrinone electric dipole transition moments have a chiral, helical relative orientation [40]. For the "oblique" conformers, exciton coupling theory thus predicts intensity from both exciton transitions and hence a broadened UV–Vis absorption curve. This may be seen in the UV–Vis spectrum of **1** in $(CH_3)_2SO$ solvent, where the location (λ) and shape of the UV–Vis absorptions are very similar and are little altered in going from polar $(CH_3)_2SO$ solvent to nonpolar solvents such as chloroform and benzene—an indication that the ridge-tile conformation (or more particularly the relative orientation of the dipyrrinone electric dipole transition moments) is scarcely altered with changes in solvents.

Induced circular dichroism

Bilirubins fold in the middle into ridge-tile conformations that lie at energy minima. With the added stabilization from intramolecular hydrogen bonding, two interconverting conformational enantiomers (Fig. 1b) dominate the conformational energy map [7]. In isotropic solvents, a 50:50 mixture of enantiomers is obtained, but when a chiral complexation agent such as quinine [36] or serum albumin [37] is added, the equilibrium shifts toward either the ***M*** or ***P*** enantiomer, and in such cases one observes typically intense bisignate circular dichroism (CD) Cotton effects for the long-wavelength rubin UV–Vis electronic transitions near 400–450 nm. Such Cotton effects are associated with an exciton interaction between the rubin's two dipyrrinone chromophores that are not directly conjugated [7, 36]. And the signed order of the Cotton effects has been correlated with the relative orientation of the dipyrrinones and hence the absolute configuration ***M*** or ***P*** of the rubin [7, 36].

The CD spectra of **1**–**3** in human serum albumin (HSA) (Fig. 4) show an intense negative long-wavelength Cotton effect, indicating that HSA binds predominantly the ***M*** enantiomer. As the MPEG chain length increases, the magnitude of the Cotton effect decreases, suggesting that the binding ability of HSA decreases as the MPEG chain length increases. Presumably, the bilirubin binding pocket

Table 5 Comparison of the solvent dependence of the UV–Vis spectral data of MPEG rubins **1**–**4** with mesobilirubin-XIIIα (MBR) and bilirubin (BR)

Compounds	ε^{max} (λ^{max}, nm)						
	Benzene	$CHCl_3$	$(CH_3)_2CO$	CH_3OH	CH_3CN	$(CH_3)_2SO$	H_2O (2% DMSO)
1	60,600 (423)	59,100 (421)	60,400 (416)	61,300 (412)	58,900 (414)	62,700 (415)	49,200 (420)
				49,500 (383)[a]		55,400 (383)[a]	42,900 (392)[a]
2	57,900 (423)	59,000 (420)	58,300 (415)	60,200 (413)	58,600 (415)	61,400 (415)	45,100 (419)[a]
				48,500 (383)[a]		51,500 (383)[a]	48,100 (397)
3	58,300 (423)	58,200 (421)	56,700 (416)	59,100 (413)	57,000 (415)	60,200 (415)	46,400 (410)
				46,700 (383)		50,200 (383)	45,100 (421)
4	51,800 (421)	52,700 (419)	51,900 (414)	54,400 (412)	51,300 (413)	54,300 (415)	Insol
				32,500 (382)[a]		44,800 (381)[a]	
MBR	49,000 (439)	50,300 (431)	49,700 (427)	50,600 (425)	49,000 (425)	52,500 (428)	Insol
BR	45,800 (447)	46,920 (450)	47,600 (447)	45,300 (446)	47,000 (445)	47,800 (446)	Insol
			34,600 (415)[a]	37,500 (416)[a]	39,400 (417)[a]	37,700 (415)[a]	

At 22 °C in concentrations $\sim 1.4 \times 10^{-5}$ M, λ^{max} in nm, ε^{max} in $dm^3\ mol^{-1}\ cm^{-1}$; 2% (by vol) $CHCl_3$ present in all solvents

[a] Shoulders (or) inflections were determined by first- and second-derivative spectra

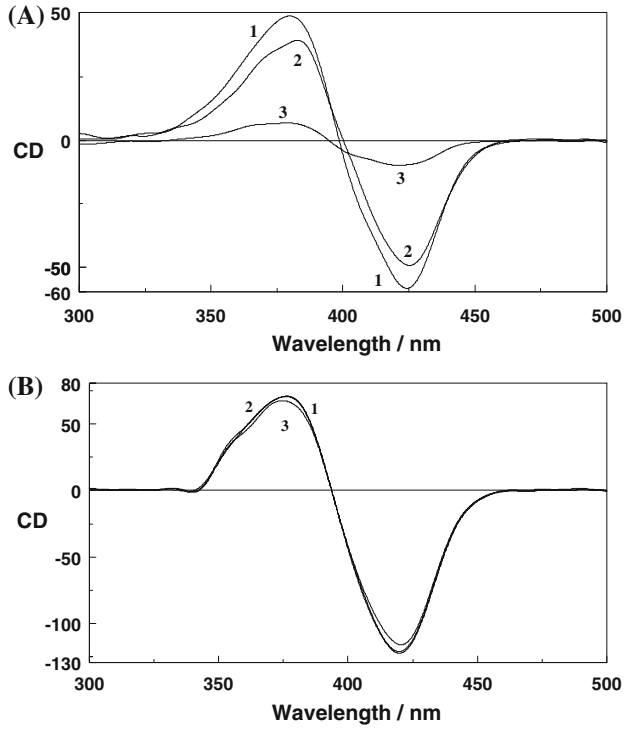

Fig. 4 Comparison of the RT CD and UV–Visible spectroscopic data of **1**, **2**, and **3** in **a** pH 7.4 aqueous 0.1 M Tris-buffered HSA (pigment conc. $\sim 2 \times 10^{-5}$ M, HSA conc. $\sim 4 \times 10^{-5}$ M). **b** CH_2Cl_2 solutions containing quinine (pigment conc. $\sim 2 \times 10^{-5}$ M; quinine conc. $\sim 6 \times 10^{-3}$ M; pigment:quinine molar ratio = ~1:300). In (**a**), **1**, $\Delta\varepsilon_{383(max)} = 49$, $\Delta\varepsilon_{400} = 0$, $\Delta\varepsilon_{425(max)} = -59$, UV–Vis $\varepsilon_{(421)max} = 57{,}600$; **2**, $\Delta\varepsilon_{380(max)} = 39$, $\Delta\varepsilon_{399} = 0$, $\Delta\varepsilon_{424(max)} = -50$, UV–Vis $\Delta\varepsilon_{(415)max} = 58{,}100$; and **3**, $\Delta\varepsilon_{379(max)} = 7.0$, $\Delta\varepsilon_{395} = 0$, $\Delta\varepsilon_{421(max)} = 10$, UV–Vis $\Delta\varepsilon_{(416)max} = 57{,}800$. In (**b**): **1**, $\Delta\varepsilon_{376(max)} = 70$, $\Delta\varepsilon_{394} = 0$, $\Delta\varepsilon_{421(max)} = -122$, UV–Vis $\Delta\varepsilon_{(421)max} = 54{,}100$; **2**, $\Delta\varepsilon_{376(max)} = 70$, $\Delta\varepsilon_{394} = 0$, $\Delta\varepsilon_{420(max)} = -125$, UV–Vis $\Delta\varepsilon_{(420)max} = 55{,}400$; and **3**, $\Delta\varepsilon_{376(max)} = 66$, $\Delta\varepsilon_{394} = 0$, $\Delta\varepsilon_{421(max)} = -117$, UV–Vis $\varepsilon_{(420)max} = 54{,}900$

on HSA cannot selectively accommodate the increased spatial demand by the even larger MPEG groups attached to the lactam rings. However, no such limits are placed on the ability of quinine to displace the conformational enantiomers toward ***M*** (Fig. 4b). Here the CD spectra of **1**–**3** are nearly indistinguishable.

As expected from earlier studies with bilirubin [38], the CD Cotton effects from **1** on HSA are strengthened upon addition of small quantities of $CHCl_3$ but are not inverted (Table 6). In contrast, the CD intensities of **2** and **3** decrease (strongly for **2**) but do not invert. Here again, the CD data point to a weakened ability of these HSA solutions to exhibit enantioselective binding.

Concluding comments

New tetra-MPEGylated biliruinoids (**1**–**3**) were synthesized with short polyethyleneglycol methyl ether chains on the lactam rings. The pigments were fully soluble in $CHCl_3$ and in CH_3OH (in which bilirubin is insoluble) and exhibited partial water solubility. While the solubility in $CHCl_3$ and CH_3OH was sufficient for determining that the pigments were monomers in these solvents, it was insufficient for VPO in H_2O. ^1H NMR experiments confirmed the intramolecular hydrogen-bonded ridge-tile conformations in $CDCl_3$, and the NH chemical shift data were consistent with the same in H_2O (in which we used water-suppression techniques). Although the aqueous solubility of **3** was insufficient for either VPO or pK_a studies, it seems reasonable to assume that, with only slightly longer MPEG chains, e.g., tetraethyleneglycol or pentaethyleneglycol, the pigment would have sufficient water solubility for both measurements.

Solubility in CH_3OH (unlike bilirubin, which is insoluble) was sufficient for measuring the pK_a values for the propionic carboxyl groups by vacuum-assisted multiplexed capillary electrophoresis (VAMCE) [39] in H_2O-CH_3OH (30–60%). The highly reliable Yesuda-Shedlovsky extrapolation [40–42] to pure water yielded pK_a values of ~4.9 for **1**–**4**, as estimated for bilirubin [18] and measured for nonaggregated carboxyl groups.

Experimental

All nuclear magnetic resonance (NMR) spectra were obtained on a Varian 500 MHz (^1H) and 125 MHz (^{13}C), respectively, in deuteriochloroform unless otherwise indicated. Chemical shifts are reported in ppm, referenced to the residual chloroform proton signal at 7.26 ppm and ^{13}C signal at 77.23 ppm unless otherwise noted. Melting points were taken on a Mel-Temp capillary apparatus and are reported corrected. Elemental analyses, obtained from Desert Analytics, Tucson, AZ, were within ±0.4% of the calculated values. All UV–Vis spectra were recorded on a Perkin-Elmer λ-12 spectrophotometer. Vapor pressure osmometry (VPO) measurements were performed on an OSMOMAT 070-SA instrument (Gonotech GmbH, Germany) in HPLC-grade $CHCl_3$ (Fisher) at 45 °C. Analytical thin-layer chromatography (TLC) was carried out on J.T. Baker silica gel IB-F plates (125 μm layer). Flash column chromatography was carried out using 60–200 mesh silica gel (M. Woelm, Eschwege). For final purification, radial chromatography was carried out on 1- or 2-mm-thick rotors of Merck silica gel PF_{254} with calcium sulfate binder, preparative layer grade, using a Chromatotron (Harrison Research, Inc., Palo Alto, CA, USA). All solvents were reagent grade obtained from Fisher-Acros.

The spectral data were obtained in spectral-grade solvents (Aldrich or Fisher). 2,3,17,18-Tetramethoxybilirubin (**4**) [19] and pyrrolinones **6**–**8** were available from previous

Table 6 Changes in CD data of **1–3** following addition of trace amounts of $CHCl_3$ to pH 7.4 Tris-buffered aqueous HSA solutions of **1–3**

$CHCl_3$ added (mm^3)	**1**			**2**			**3**		
	$\Delta\varepsilon^{max}$ (λ_1)	$\Delta\varepsilon = 0$ (λ_2)	$\Delta\varepsilon^{max}$ (λ_3)	$\Delta\varepsilon^{max}$ (λ_1)	$\Delta\varepsilon = 0$ (λ_2)	$\Delta\varepsilon^{max}$ (λ_3)	$\Delta\varepsilon^{max}$ (λ_1)	$\Delta\varepsilon = 0$ (λ_2)	$\Delta\varepsilon^{max}$ (λ_2)
0	+49 (393)	400	−59 (425)	+39 (380)	99	−50 (425)	+7 (379)	395	−10 (421)
1	+52 (380)	398	−68 (424)	+35 (380)	399	−41 (425)	+5 (379)	395	−7 (424)
3	+590 (380)	398	−81 (424)	–	–	–	–	–	–
5	+62 (379)	398	−86 (424)	+33 (378)	399	−39 (425)	+5 (380)	395	−6 (425)
7	+68 (379)	398	−96 (424)	–	–	–	–	–	–
10	+78 (379)	397	−115 (423)	–	–	–	–	–	–
15	+87 (379)	397	−129 (424)	+27 (381)	399	−34 (425)	–	–	–
20	+90 (379)	397	−136 (424)	–	–	–	–	–	–
35	–	–	–	+15 (380)	398	−21 (425)	–	–	–
45	–	–	–	+10 (375)	398	−16 (424)	–	–	–
65	–	–	–	+6 (371)	398	−13 (424)	–	–	–
100	–	–	–	+2 (364)	392	−3 (421)	–	–	–

0.1 M Tris buffer with 2×10^{-5} M **1–3** + 4×10^{-5} M HSA

HSA human serum albumin

work. Dipyrroledialdehyde **5** [17] was synthesized according to the literature method.

Solubility in H_2O and CH_3OH

In order to compare the aqueous solubility of **1–4**, stock solutions of each were prepared in $CHCl_3$ and in $(CH_3)_2SO$ solvents. Measured aliquots were withdrawn and diluted in 5.00 cm^3 volumetric flasks with CH_3OH or H_2O to create $\sim$1–3 $\times$ 10^{-5} M pigment solutions in CH_3OH-2% $CHCl_3$ and in H_2O-2% $(CH_3)_2SO$. The UV–visible absorbances of each were determined ($\sim$30,000), and the solvent was removed to dryness. Then pure CH_3OH was added to the residue from evaporation of CH_3OH-2% $CHCl_3$ solutions, and pure H_2O (pH 7) was added to the residue from evaporation of the 10^{-5} M $CHCl_3$ solutions. After digestion by ultrasonication and centrifugation, the absorbances of the reconstituted CH_3OH and H_2O solutions were determined and compared with those of the original $\sim$1–3 $\times$ 10^{-5} M solutions in order to determine the pigment concentrations.

UV and CD measurements

Stock solutions of **1–3** ($\sim 7.0 \times 10^{-4}$ M) were prepared by dissolving an appropriate amount of the desired pigment in 1.0 cm^3 of $(CH_3)_2SO$ and $CHCl_3$. Next, a 0.10 cm^3 aliquot of the stock solution was diluted to 5 cm^3 (volumetric flask) with the specified organic solvent for UV–Vis studies (Table 3) or, for CD studies involving human serum albumin (HSA), with an HSA solution ($\sim 4 \times 10^{-5}$ M in pH 7.4 Tris buffer). The final concentration of the solution was $\sim 2 \times 10^{-5}$ M in pigment. Up to four 5 cm^3 solutions of each pigment were prepared, as needed, in 5-cm^3 volumetric flasks. For CD studies in $CHCl_3$, solutions were prepared directly in $CHCl_3$ containing a 300:1 molar ratio of quinine:pigment to give final concentrations of $\sim 2 \times 10^{-5}$ M in pigment.

2,17-Di(desmethyl)-3,18-di(desvinyl)-2,3,17,18-tetrakis (2-methoxyethoxy)bilirubin (**1**, $C_{39}H_{56}N_4O_{14}$)

Pyrroledialdehyde **5** (500 mg, 1.20 mmol) and 1.07 mg pyrrolinone **6** (4.60 mmol) were dissolved in 6 cm^3 acetonitrile in a pressure tube. To this solution was added 0.8 cm^3 1,8-diazabicyclo[5.4.0]undec-7-ene (DBU, 4–5 eq.), and the reaction mixture was heated at 120–130 °C under N_2 atmosphere for 10 days. After evaporating the solvent, the residue was dissolved in CH_2Cl_2, and washed with water and then with 5% aq. HCl. The organic layer was dried and evaporated (roto-vap), and the residue was purified: first by flash chromatography using 98:2 (by vol) CH_2Cl_2:CH_3OH, then by radial chromatography using 5:2–1:1 (by vol) *n*-hexane:ethyl acetate in gradient. The combined fractions were evaporated (roto-vap) to yield pure **1**. Yield: 260 mg (28%); m.p.: 212–213 °C; ^{1}H NMR: δ = 2.13 (s, 6H), 2.53-3.00 (m, 8H), 3.37 (s, 6H), 3.41 (s, 6H), 3.61 (m, 4H), 3.68 (m, 4H), 4.02 (s, 2H), 4.25 (m, 4H), 4.55 (m, 4H), 6.24 (s, 2H), 8.99 (brs, 1H), 10.31 (brs, 2H), 13.09 (brs, 2H) ppm; ^{13}C NMR: δ = 10.3, 18.7, 22.4, 32.8, 59.0, 59.3, 71.3, 71.5, 71.6, 71.8, 100.6, 119.4, 120.8, 123.9, 124.1, 125.3, 133.2, 147.6, 169.3, 179.8 ppm.

2,17-Di(desmethyl)-3,17-di(desvinyl)-2,3,17,18-tetrakis [2-(2-methoxyethoxy)ethoxy]bilirubin (**2**, $C_{47}H_{72}N_4O_{18}$)
Following the procedure above, 350 mg **5** (0.820 mmol) and 1.04 mg **7** (3.30 mmol) in 6 cm^3 dry acetonitrile in a pressure tube were reacted in the presence of 0.8 cm^3 DBU (4–5 eq.) at 120–130 °C under N_2 for 10 days and 10 h. After workup and chromatographic purification (as above) pure **2** was isolated. Yield: 100 mg (13%); m.p.: 182–184 °C (melted with decomp); ^{1}H NMR: $\delta = 2.13$ (s, 6H), 2.53–3.00 (m, 8H), 3.36 (s, 6H), 3.37 (s, 6H), 3.52–3.79 (m, 24H), 4.02 (s, 2H), 4.26 (m, 4H), 4.59 (m, 4H), 6.22 (s, 2H), 8.99 (brs, 1H), 10.20 (brs, 2H), 13.14 (brs, 2H) ppm; ^{13}C NMR: $\delta = 10.3$, 18.7, 22.4, 32.8, 59.2, 59.3, 70.2, 70.3, 70.6, 70.9, 71.4, 71.6, 71.8, 72.1, 72.2, 100.5, 119.3, 120.9, 123.8, 124.0, 125.2, 133.2, 147.7, 169.4, 179.7 ppm.

2,3-Di(desmethyl)-3,17-di(desvinyl)-2,3,17,18-tetrakis [2-[2-(2-methoxyethoxy)ethoxy]ethoxy]bilirubin (**3**, $C_{55}H_{88}N_4O_{22}$)
As above 500 mg (1.20 mmol) pyrroledialdehyde **5** and 2.83 mg pyrrolinone **8** (7.20 mmol) were dissolved in 6 cm^3 dry acetonitrile in a pressure tube and converted to **3** following addition of 2.0 cm^3 DBU (12 eq.) and heating at 120–130 °C under N_2 for 10 days. Yield: 30 mg (4.5%); m.p.: 102–104 °C; ^{1}H NMR: $\delta = 2.12$ (s, 6H), 2.53–3.00 (m, 8H), 3.35 (s, 6H), 3.36 (s, 6H), 3.52–3.79 (m, 40H), 4.01 (s, 2H), 4.25 (m, 4H), 4.57 (m, 4H), 6.21 (s, 2H), 8.99 (brs, 1H), 10.19 (brs, 2H), 13.14 (brs, 2H) ppm; ^{13}C NMR: $\delta = 10.3$, 18.7, 22.4, 32.8, 59.2, 59.3, 70.17, 70.25, 70.66, 70.75, 70.79, 70.84, 70.86, 70.95, 71.36, 71.4, 71.85, 72.13, 72.14, 100.4, 119.3, 120.9, 123.7, 124.1, 125.2, 133.1, 147.6, 169.4, 179.7 ppm.

Acknowledgments We thank the US National Institutes of Health (HD 17779) for generous support of this work and the National Science Foundation (CHE-0521191) for providing funding for acquisition of a 400-MHz NMR spectrometer and upgrade of our 500-MHz NMR. We thank Prof. A.F. McDonagh (Univ. California, San Francisco) for running the HPLCs of **1**–**4**. We also thank Prof. T.W. Bell for use of the VPO apparatus and Dr. Stephen Spain for assistance with the water-suppression NMR experiments. We thank Ms. Jolanta Plewa and Dr. Christopher Welch of Merck Research Labs for the VAMCE measurements of pK_a.

References

1. Chowdhury JR, Wolkoff AW, Chowdhury NR, Arias IM (2001) Hereditary jaundice and disorders of bilirubin metabolism. In: Scriver CF, Beaudet AL, Sly WS, Valle D (eds) The metabolic and molecular bases of inherited disease, chap 125, McGraw-Hill, New York, pp 3063–3101
2. Lightner DA, McDonagh AF (1984) Acc Chem Res 17:417
3. McDonagh AF, Lightner DA (1985) Pediatrics 75:443
4. McDonagh AF (1979) Bile pigments: Bilatrienes and 5,15-biladienes. In: Dolphin D (ed) The porphyrins, chap 6, vol VI, Academic Press, New York
5. Schmid R, McDonagh AF (1978) Hyperbilirubinemia. In: Stanbury JB, Wyngarden JB, Fredrickson DS (eds) Basis of inherited disease, 4th edn. McGraw-Hill, New York
6. Falk H (1989) The chemistry of linear oligopyrroles and bile pigments. Springer, Wien
7. Person RV, Peterson BR, Lightner DA (1994) J Am Chem Soc 116:42
8. Bonnett R, Davies JE, Hursthouse NB, Sheldrick GM (1978) Proc R Soc London Ser B 202:249
9. LeBas G, Allegret A, Mauguen Y, DeRango C, Bailly M (1980) Acta Crystallogr Sect B 36:3007
10. Becker W, Sheldrick WS (1978) Acta Crystallogr Sect B 34:1298
11. Sheldrick WS (1983) Israel J Chem 23:55
12. Sheldrick WS (1976) J Chem Soc Perkin 2, 1457
13. Brodersen R (1986) Aqueous solubility, albumin binding, and tissue distribution of bilirubin. In: Ostrow JD (ed) Bile pigments and jaundice. Marcel Dekker, New York, pp 157–181
14. Brodersen R (1979) J Biol Chem 254:2364
15. Ghosh B, Lightner DA, McDonagh AF (2004) Monatsh Chem 135:1189
16. Xie M, Holmes DL, Lightner DA (1993) Tetrahedron 49:9235
17. Brower JO, Lightner DA, McDonagh AF (2000) Tetrahedron 56:7869
18. Boiadjiev SE, Watters K, Lai B, Wolf S, Welch W, McDonagh AF, Lightner DA (2004) Biochemistry 43:15617
19. Dey SK, Lightner DA (2008) J Org Chem 73:2704
20. Dey SK, Lightner DA (2009) Monatsh Chem 140:161
21. Boiadjiev SE, Lightner DA (1994) Synlett 777
22. Boiadjiev SE, Lightner DA (2006) Org Prep Proced Int 38:347
23. Brower JO, Lightner DA, McDonagh AF (2001) Tetrahedron 57:7813
24. Brower JO, Lightner DA (2001) Monatsh Chem 132:1527
25. Brower JO, Huggins MT, Boiadjiev SE, Lightner DA (2000) Monatsh Chem 131:1047
26. Huggins MT, Lightner DA (2000) J Org Chem 65:6001
27. Boiadjiev SE, Anstine DT, Lightner DA (1995) J Am Chem Soc 117:8727
28. Boiadjiev SE, Anstine DT, Maverick E, Lightner DA (1995) Tetrahedron Asymmetry 6:2253
29. Nogales DF, Ma J-S, Lightner DA (1993) Tetrahedron 49:2361
30. Navon G, Frank S, Kaplan D (1984) J Chem Soc Perkin 2, 1145
31. Tipton AK, Lightner DA, McDonagh AF (2001) J Org Chem 66:1832
32. Ghosh B, Lightner DA (2003) J Heterocycl Chem 40:1113
33. Kasha M, El-Bayoumi MA, Rhodes W (1961) J Chim Phys Chim Biol 58:916
34. Falk H, Vormayr G, Margulies L, Metz S, Mazur Y (1986) Monatsh Chem 117:849
35. Falk H, Grubmayr K, Höllbacher G, Hofer O, Leodolter A, Neufingerl F, Ribó JM (1977) Monatsh Chem 108:1113
36. Lightner DA, Gawroński JK, Wijekoon WMD (1987) J Am Chem Soc 109:6354
37. Lightner DA, Wijekoon WMD, Zhang MH (1988) J Biol Chem 263:16669
38. Pu Y-M, McDonagh AF, Lightner DA (1993) J Am Chem Soc 115:377
39. Shalaeva M, Kenseth J, Lombardo F, Bastin A (2008) J Pharm Sci 97:2581
40. Yesuda M (1959) Bull Chem Soc Jpn 32:429
41. Shedlovsky T (1962) In: Pesce B (ed) Electrolytes. Pergamon, New York
42. Avdeef A, Box KJ, Comer JEA, Gilges M, Hadley M, Hibbert C, Patterson W, Tam KY (1999) J Pharm Biomed Anal 20:632